PROCEEDINGS OF SCIENCE

An all-sky search method for coherent magnetic field deflections of ultra-high-energy cosmic rays based on deep learning

Josina Schulte,[a,*] **Teresa Bister**[b,c] **and Martin Erdmann**[a]

[a] *RWTH Aachen University, III. Physikalisches Institut A, Otto-Blumenthal-Str., 52074 Aachen, Germany*

[b] *Institute for Mathematics, Astrophysics and Particle Physics, Radboud Universiteit Nijmegen, Nijmegen, The Netherlands*

[c] *Nationaal Instituut voor Kernfysica en Hoge Energie Fysica (NIKHEF), Science Park, Amsterdam, The Netherlands*

E-mail: josina.schulte@rwth-aachen.de

We present a method for reconstructing coherent deflections of ultra-high-energy cosmic ray arrival directions that are expected from propagation through cosmic magnetic fields. Concretely, we apply a data-driven approach that searches for deflection patterns simultaneously in every sky direction from the individual cosmic ray arrival directions and energies that can be measured, for example, at the Pierre Auger Observatory. For that, we parameterize the deflections using a spherical harmonic expansion in combination with a variable magnetic field strength. The coefficients for the field orientations and strengths are adapted using a likelihood-free Bayesian approach based on normalizing flows. This allows for a straightforward assessment of the uncertainty on the predicted deflection in every sky direction. We evaluate the method's sensitivity to identify and parameterize the presence of coherent magnetic field deflections on realistic simulated astrophysical scenarios.

38th International Cosmic Ray Conference (ICRC2023)
26 July - 3 August, 2023
Nagoya, Japan

ICRC2023
38th International Cosmic Ray Conference
The Astroparticle Physics Conference

*Speaker

PoS(ICRC2023)198

1. Introduction

One of the most intriguing open questions in astroparticle physics to date is the origin of ultra-high-energy cosmic rays (UHECRs). The arrival direction distribution of these particles could unveil information on their source directions. However, the influence of magnetic fields, especially the Galactic magnetic field (GMF), disturbs the direct path of the charged particles from the sources to Earth. Consequently, the conclusions drawn from the measured UHECR arrival directions must be evaluated in light of information about the GMF. With detailed knowledge of the GMF impact and the individual energies and charges of the incoming cosmic rays, the origin of the UHECRs could be traced. But, the Galactic magnetic field is not yet well constrained, resulting in different models. As for cosmic ray data, observatories such as the Pierre Auger Observatory allow us to measure the properties of extended air showers induced by UHECRs. These provide information on the direction of arrival, the energy, and the mass of the cosmic rays. An analysis of the arrival directions measured at the Pierre Auger Observatory has unveiled a correlation with a catalog of starburst galaxies [1, 2]. An interpretation of this result is however difficult without explicit knowledge of cosmic-ray charges and the Galactic magnetic field effect. Therefore, we include the effects of an adaptable Galactic magnetic field in the analysis of the arrival directions using a data-driven approach. In particular, we focus on coherent magnetic field deflections, since their signatures can help to identify possible source directions. Here, we will investigate simulated astrophysical scenarios with a fixed source hypothesis, namely the starburst galaxy catalog of [1]. This allows us to evaluate the sensitivity of statements about the coherent magnetic field within the frame of that source hypothesis.

2. Method for reconstructing coherent deflections

To model the coherent magnetic field deflections of UHECRs in a generic and continuous way, we parameterize the resulting deflection directions and strengths as a function of the direction in the sky by an expansion in spherical harmonics. By limiting the degree of the spherical harmonics expansion, the size of regions of similar coherent deflections can be specified. For estimating the adaptable parameters we employ a likelihood-free Bayesian inference method based on deep learning.

2.1 Modeling of the coherent magnetic field deflections

We use real spherical harmonics $Y_{l,m}$ of degree l and order m with the corresponding expansion coefficients $a_{l,m}$:

$$\Psi(\theta, \phi) = \sum_{l=0}^{l_{\max}} \sum_{m=-l}^{m=l} a_{l,m} Y_{l,m}(\theta, \phi) \tag{1}$$

to parameterize the deflection direction $\Psi(\theta, \phi)$ and, similarly, the deflection strength $\delta(\theta, \phi)$ as a function of the direction in the sky, defined by the spherical angular coordinates θ, ϕ. For the deflection direction $\Psi(\theta, \phi)$, following [3], the maximum degree $l_{\max} = 5$ is chosen, corresponding to 36 free parameters. Here, the deflection direction is defined with respect to a fixed vector field tangent to the celestial sphere. The range of possible values is between 0° and 360°. Currently,

the Galactic meridians are chosen as the reference point for 90°. One alternative definition could rely on a specific Galactic magnetic field model. The expansion of the spherical harmonics would then reflect deviations from the original assumption. For the parameterization of the strength of the Galactic magnetic field $\delta(\theta, \phi)$, we choose $l_{\max} = 2$, where the choice of the degree could be easily adapted in future work. The values of the spherical harmonics expansion then reflect the deflection strength δ scaled by the rigidity R of the cosmic ray. The chosen bounds are $0°/(R/\mathrm{EV})$ and $200°/(R/\mathrm{EV})$.

2.2 Deep-learning based analysis framework

The reconstruction of the parameters $a_{l,m}$ is performed with likelihood-free Bayesian inference using normalizing flows [4], a technique based on deep learning. With this, the posterior distributions $p(\theta|y)$ of parameters θ under the condition of observables y can be inferred [5], providing estimates for the parameters as well as their uncertainties. For this purpose, a bijective mapping between the specific posterior distribution and a simple distribution is established, which is represented by a neural network, namely a normalizing flow. This neural network is based on invertible blocks, which receive the condition, i.e., the observables, as additional input. During training, a loss function describing the distance between the learned posterior distribution and the true posterior distribution is minimized. For evaluation, the trained network outputs the posterior distribution of the parameters under the condition of specific observables. We already demonstrated the abilities of this method for the inference of cosmic-ray source properties with energy spectrum and depth of shower maximum distributions, where we achieved comparable results to the frequently used Markov Chain Monte Carlo method [5]. The advantage of the deep-learning-based approach is the fast inference, which is suited for extensive testing of the method, and the possibility to preprocess the observables with an additional neural network owing to the likelihood-free approach. In this contribution, the framework is adapted to manage the arrival directions and energies of cosmic rays as observables. For intricate observables such as these, we use the ability to preprocess the input by means of an additional neural network to generate a suitable representation of the observables. In this case, instead of employing the measured observables directly, the appropriate representation from the additional neural network is given as conditional input to the invertible blocks of the normalizing flow. The weights of the network, which determines the appropriate representation of the observables, are adapted during the training simultaneously with the weights of the normalizing flow via the loss function of the latter. For our application of arrival directions as well as the individual energies of the cosmic rays, we have chosen an efficient transformer, the Nyströmformer [6], as a pre-network. The idea of this approach is based on the idea of attention [7], which is fundamental for transformers and provides a measure for the connection between the inputs. In our use case, the transformer should assign high attention to cosmic rays from the same sources. Ideally, coherently deflected cosmic rays can be identified. In our setup of the transformer, no positional encoding is used as the problem does not depend on the order of the cosmic rays. The actual position is already encoded in the coordinates of the arrival directions, x, y, z. Therefore, we only use a learnable embedding which is applied on the coordinates, x, y, z, and a scaled energy of the cosmic rays, $\log(E/\,\mathrm{eV}) - 19.2$.

2.3 Simulation setup

The simulations are based on two components: a homogeneous and isotropic background contribution and a contribution from the catalog sources. The cosmic rays originating from the homogeneous and isotropic background are distributed according to the exposure of the Pierre Auger Observatory [8]. In this isotropic case, no coherent magnetic field deflections have to be considered due to Liouville's theorem. The energies and charges of all cosmic rays are simulated to follow the results of [9] for the case of SBGs as potential source candidates. For the cosmic rays from the source catalog, namely the SBGs [1], Galactic magnetic field effects have to be taken into account. First, the influence of the turbulent component of the Galactic magnetic field is modeled by a blurring of the arrival directions with a Fisher distribution of width $20^\circ/(R/\mathrm{EV})$ [3]. Following, the coherent Galactic magnetic field influence is simulated. For this, the coefficients of the spherical harmonics expansion $a_{l,m}$ for the deflection direction and strength model are selected. Here, all cosmic rays attributed to a source receive the deflection direction at the respective source's position $\Psi(\theta_{\mathrm{source}}, \phi_{\mathrm{source}})$ while the angular distance to the source follows the deflection strength $\delta(\theta_{\mathrm{source}}, \phi_{\mathrm{source}})$ scaled by the inverse cosmic-ray rigidity. As in [9], the detected energy threshold is set to $10^{19.2}$ eV. Following the event statistics of the Pierre Auger Observatory, the number of cosmic rays above this threshold is on the order of 12k. The signal fraction is chosen to be 2%, corresponding to a total of 240 cosmic rays from the SBGs. Using various combinations of $a^{\Psi}_{l,m}$ and $a^{\delta}_{l,m}$, many simulations are created to produce training, validation, and test data. In Fig. 1, an exemplary simulation from the test data set is shown. On the upper left, the deflection direction map is presented. The colors depict the deflection angle $\Psi(\theta, \phi)$, defined with respect to the Galactic meridians. On the upper right, the deflection strength map is depicted. The lightness represents the deflection strength $\delta(\theta, \phi)$ for a $R = 1$ EV particle, varying over the sky. The resulting arrival directions are shown in the lower part of Fig. 1. Elongated patterns of cosmic rays following their rigidity are present around the catalog sources. Also, the influence of the turbulent magnetic field is visible by the smearing of the patterns.

3. Application of method on simulated astrophysical scenarios

In this section, the application of the method on the simulated data set shown in Fig. 1 is discussed. We obtain posterior distributions of the spherical harmonics expansion coefficients $a^{\Psi}_{l,m}$ and $a^{\delta}_{l,m}$ by using the arrival directions and the corresponding energies as conditional input to the neural network setup described in sec. 2.2. From the posterior distributions, the reconstructed deflection angles and strengths can be inferred. On the one hand, we use the mean of the posterior distributions of the parameters to reconstruct the most probable deflections Ψ and strengths δ as a function of θ, ϕ. On the other hand, calculating deflection maps for many values drawn from the posterior distributions allows us to assess the corresponding directional uncertainties. To this end, the standard deviation of the value of $\Psi(\theta, \phi)$ and $\delta(\theta, \phi)$ is calculated. These measures are depicted in Fig. 2 and Fig. 3, respectively. In Fig. 2, the result for the deflection angle $\Psi(\theta, \phi)$ reconstruction is visualized. On the left, the mean estimate shows a quite homogeneous distribution. When evaluating this map more closely, an agreement of the values at the positions of the strong catalog sources is observed. Around NGC4945 and NGC1068, the deflection angle estimate corresponds to the 245° and 204°, respectively, agreeing within 16° and 12° with the

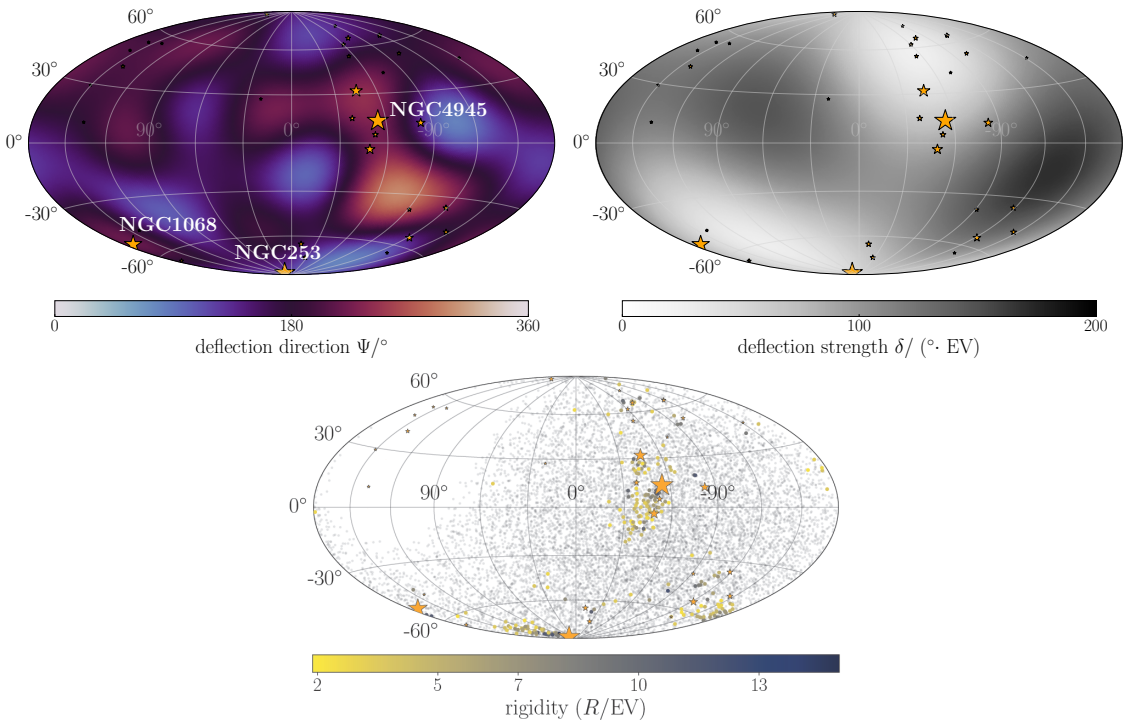

Figure 1: Exemplary simulation from the test data set. All maps are in Galactic coordinates and the positions of the catalog sources are given by the star symbols whereby the size is proportional to the arriving cosmic-ray flux. Upper row: simulated deflection direction $\Psi(\theta, \phi)$ (left) and strength $\delta(\theta, \phi)$ (right) maps. Lower row: resulting arrival directions for the deflection maps. Background cosmic rays are depicted as grey dots, and cosmic rays from the catalog sources are colored according to their rigidity.

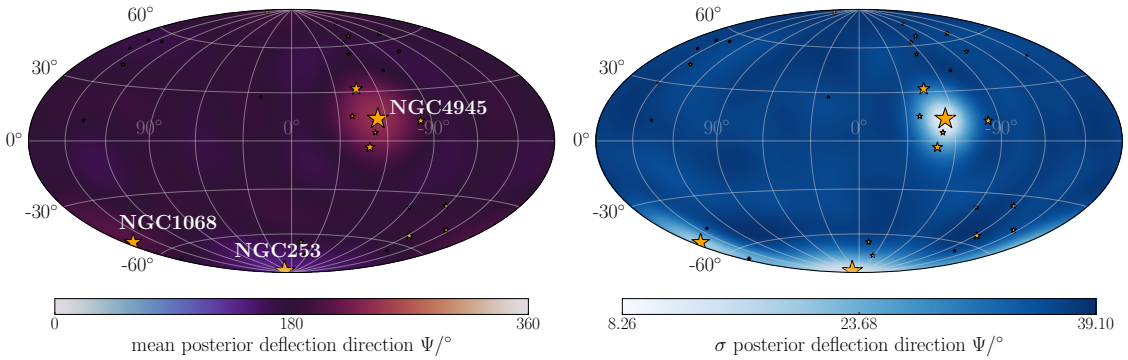

Figure 2: Reconstructed deflection direction $\Psi(\theta, \phi)$ (left) and uncertainty on it (right) for the exemplary simulation from Fig. 1.

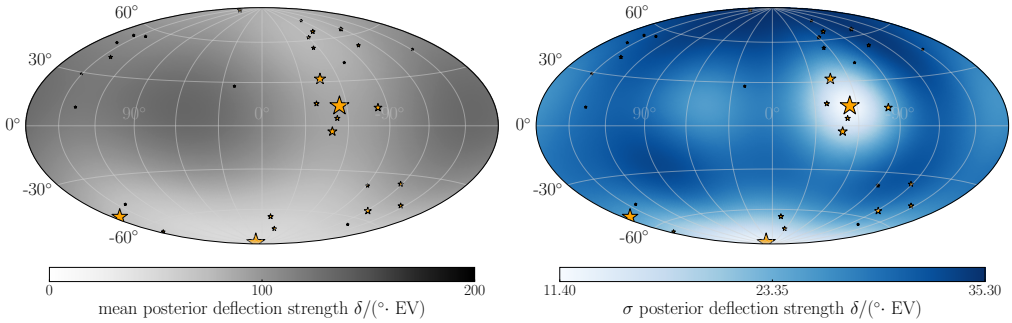

Figure 3: Reconstructed deflection strength $\delta(\theta, \phi)$ (left) and uncertainty (right) for the exemplary simulation from Fig. 1.

simulated truth, compare to Fig. 1. The deflection angle agreement in the south at NGC253 is also visually present with a lighter shade of purple, corresponding to 142° for the reconstruction versus 121° for the simulation, compare Fig. 2 and Fig. 1. The corresponding uncertainty map in the upper right corner of the figure reflects these findings. The uncertainty around the named strong sources is small, whereas the uncertainty is large over the remaining sky. This map also shows the advantage of the method because, at locations without catalog sources, the large uncertainty present in the map adequately reflects that no statement about the directional deflection of cosmic rays can be made. In Fig. 3, the same metrics are shown for the reconstruction of the deflection strength $\delta(\theta, \phi)$. Again, an agreement with Fig. 1 at the positions of stronger sources is seen, especially the lower deflection strength around NGC4945, and the strengths in the Galactic south are well reconstructed. Analogously, the uncertainty map for the deflection strength shows similar behavior to the uncertainty map for the deflection direction, with small uncertainties around the strong sources and large uncertainty in the remaining sky.

4. Evaluation of sensitivity

The results from the demonstrated exemplary scenario are promising. In the following, we investigate the method quantitatively by analyzing a test data set of size 5000 with varying $a_{l,m}$ with the presented approach. As a measure of goodness-of-fit, we first analyze the absolute reconstruction quality in three different directions. The directions are chosen to include catalog sources with varying fluxes: NGC4945 is the strongest source of the catalog, NGC1068 contributes with a flux about half of the strongest source and NGC1808 is a faint source. The difference between the true deflection angle of the underlying simulation Ψ_{truth} and the reconstruction in that specific direction Ψ_{reco} for the 5000 test data sets is histogrammed and presented on the left side of Fig. 4. The distributions peak close to zero and show varying spreads depending on the flux, where the distribution of the strongest contributing source NGC4945 is the narrowest. The behavior is further evaluated in the right part of the figure by dividing the deviation at the source positions by the predicted uncertainty σ_{reco}. Here, it is apparent that the spread of $\Psi_{\mathrm{truth}} - \Psi_{\mathrm{reco}}$ in the test data equals approximately the reconstructed uncertainty σ_{reco}, being consistent with the expectation. The value for the estimated uncertainty on the weakly contributing source averaged over all test data sets is high ($\bar{\sigma}_{\mathrm{reco}} = 37.7°$) since the number of cosmic rays from this source is negligible. The uncertainty

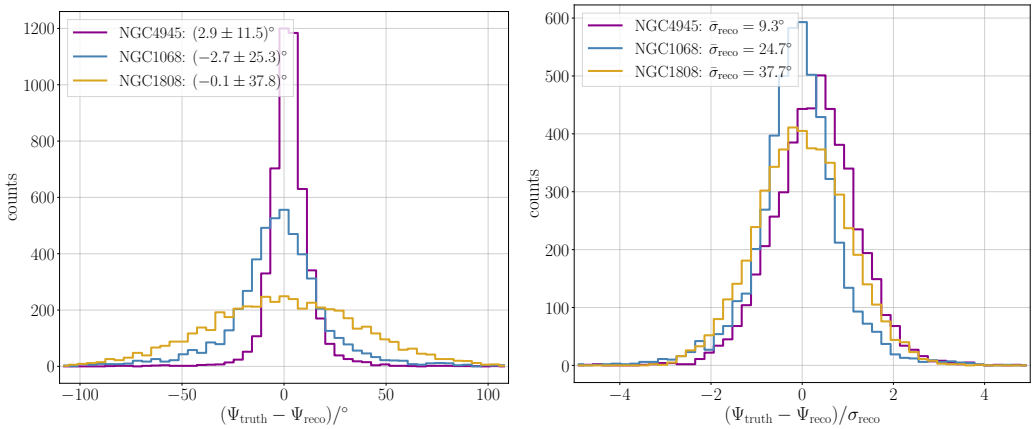

Figure 4: Difference between simulation and reconstruction of the deflection angle Ψ at the position of three different sources with varying flux weights in absolute numbers (left) and normalized to the predicted uncertainty σ_{reco} (right). The chosen sources, depicted with different colors, are the strongest source NGC4945, a medium contributing source NGC1068, and a very faint source M82.

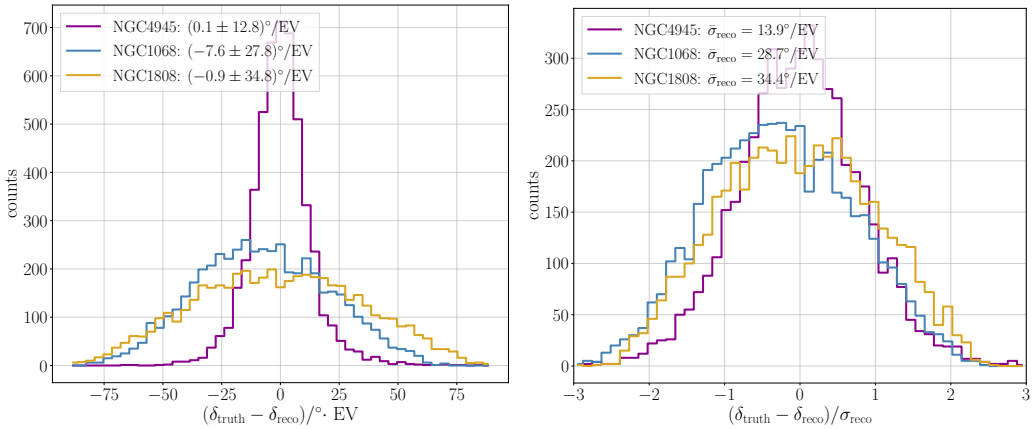

Figure 5: Same as Fig. 4, but for the deflection strength δ.

on the deflection direction of the strongest source is small for many test data sets ($\bar{\sigma}_{\text{reco}} = 9.3°$), similar to the example evaluated in the previous section. Here, the coherently deflected cosmic rays can be identified and assigned to the source.

Likewise, the results for the deflection strength are evaluated, where the same trend is visible, see Fig. 5. The coherent deflection strength in the direction of the strongest source can be predicted with an average uncertainty of 13.9°/EV. We conclude that the presented analysis method enables the reconstruction of coherent deflection direction and strength at the positions of sources from the catalog including adequate uncertainty estimation.

5. Conclusion and Outlook

In this contribution, an overview of a deep-learning-based method for the inclusion of adaptable coherent magnetic field deflections in a novel arrival directions analysis is presented. We introduce

a parameterized representation of coherent magnetic field strength and direction with spherical harmonics expansions and present the reconstruction of the parameters with a deep neural network, using the arrival directions and energies of UHECRs. The Bayesian approach to the evaluation allows us to assess a mean estimate as well as uncertainty on the prediction as a function of direction. We show detailed results on one exemplary simulation before evaluating the method on a large test data set. Our method shows good agreement between the reconstructed and simulated coherent deflection direction and strength at the catalog sources, namely the SBG catalog [1]. With this, the interpretation of the measured arrival directions and the directions of the catalog sources is extended by corresponding predictions for coherent magnetic field deflections of the cosmic rays. The reconstructed coherent magnetic field strengths unveil regions where signatures of coherent deflections are present by a small uncertainty in combination with a coherent deflection strength stronger than the turbulent one. The resulting direction of the UHECR deflection in that area is also reconstructed, again with an estimate of the uncertainty. In source regions where the turbulent component of the Galactic magnetic field dominates, either the mean estimate of the coherent deflection strength will be small or the uncertainty will be large. The predictions regarding the magnetic field influence on the UHECRs from the sources identified with this method could be compared to existing Galactic magnetic field models.

Possible extensions of the method concern the choice of the sources. In future work, the setup will be adapted to have a fixed source density resulting in varying source positions in the training data. Thus, possible source directions could light up in the uncertainty maps when applied to data. Source directions would not only be found in this analysis by identifying coherent deflection patterns but could also be located by overdensities. This can be assessed using the deflection strength map where regions with low deflection strengths combined with a small uncertainty indicate overdensities. Also, more information on the cosmic rays could be easily introduced, e.g. related to the cosmic-ray mass. The individual depth of shower maximum and the number of muons can be reconstructed now with the help of deep learning techniques, see [10–13], providing additional high-statistics information to this analysis in the near future.

References

[1] J. Biteau [for the Pierre Auger Coll.], PoS **ICRC2021** 307 (2021).
[2] P. Abreu et al. [The Pierre Auger Coll.] ApJ **935** 170 (2022).
[3] M. Wirtz et al., Eur. Phys. J. C **81**, 794 (2021).
[4] G. Papamakarios et al., Journal of Machine Learning Research **22** 57 (2021).
[5] T. Bister et al., Eur. Phys. J. C **82** 171 (2022).
[6] Y. Xiong et al., Proc. of the AAAI Conference on Artificial Intelligence **35**, 16 (2021).
[7] A. Vaswani et al., Advances In Neural Information Processing Systems **30** (2017).
[8] A. Aab et al. [The Pierre Auger Coll.], Nucl. Instrum. Methods Phys. Res. A **798** 172-213 (2015).
[9] A. Abdul Halim et al. [The Pierre Auger Coll.], submitted to JCAP, [2305.16693].
[10] A. Aab et al. [The Pierre Auger Coll.] J. Instrum. **16** P07019 (2021).
[11] A. Aab et al. [The Pierre Auger Coll.] J. Instrum. **16** P07016 (2021).
[12] N. Langner [for the Pierre Auger Coll.], these proceedings.
[13] S. Hahn [for the Pierre Auger Coll.], these proceedings.

PoS(ICRC2023)198